Schneider *et al. BMC Plant Biology* (2025) 25:1053
https://doi.org/10.1186/s12870-025-06995-9

BMC Plant Biology

RESEARCH Open Access

Holobiont-based genetic analysis reveals new plant and microbial markers for resistance against a root rot pathogen complex in pea

Michael Schneider[1*], Valentin Gfeller[1], Daniel Ariza-Suarez[2], Lukas Wille[1], Klaus H. Oldach[3], Natacha Bodenhausen[1], Martin Hartmann[4], Pierre Hohmann[1,5*], Bruno Studer[2] and Monika M. Messmer[1]

Abstract

Background The pea root rot complex is caused by various soil-borne pathogens that likely reinforce each other, influencing the composition of the root microbiome and leading to significant yield reductions. Previous studies have shown variations in the abundance of key microbial taxa and differences in disease susceptibility among plant genotypes. To better understand this relationship between plant genetics and microbiome dynamics, we conducted genetic analyses focusing on plant health and frequency of microbial taxa.

Results Two hundred fifty-two diverse pea lines were grown in naturally infested soil under controlled conditions, genotyped, assessed for their disease symptoms at the seedling stage, and analyzed the associated root microbial communities using amplicon sequencing. Genome-wide association studies (GWAS) revealed genomic loci that influence the abundance of various fungal and bacterial operational taxonomic units (OTUs). We identified 54 independent quantitative trait loci (QTLs) significantly linked to the abundance of 98 out of 1227 detected OTUs, while an additional 20 QTLs were associated with more than one OTU. The most significant region was found on chromosome 6, influencing 50 OTUs across 10 distinct QTLs.
When comparing genomic markers and microbial OTUs as predictors in a genomic prediction model for root rot resistance and seedling emergence, we found that the abundance of specific microbial groups provided a significantly better predictive ability than QTLs. The abundance of *Fusarium* species was correlated with increased infection levels, while others, such as those linked to *Dactylonectria* and *Chaetomiaceae*, positively correlated with resistance to root rot. These findings were validated by specific QTLs and high genetic heritability for OTU abundance.

Conclusion The results highlight two key points: (1) the presence and abundance of certain microbial groups in the pea root are influenced by distinct QTLs and, thus, determined by the plant genotype, and (2) these microbial communities show heritable correlations with the plant resistance to root rot. By combining plant and microbiome genetic markers—using a "holobiont" approach—we can improve predictions of root rot resistance compared to

*Correspondence:
Michael Schneider
michael.schneider@fibl.org
Pierre Hohmann
pierre.hohmann@ub.edu

Full list of author information is available at the end of the article

predictions based on plant genetics alone. These findings set a foundation for practical applications in breeding programs aimed at enhancing disease resistance through microbiome-assisted approaches.

Keywords GWAS, Microbiome, Holobiont, Pea, Genomic prediction, Pea root rot complex

Background

Legumes are crucial in shifting toward more sustainable protein production [1]. A plant-based diet not only offers environmental benefits but also reduces the risk of chronic diseases such as type 2 diabetes and cardiovascular conditions [2]. Therefore, plant-based protein sources like peas have become more and more relevant. Pea (*Pisum sativum* L.) is one of the agronomically most essential members of high-value protein crops, with a total dry seed production of six million tons in 2021 in Europe [3]. Like other legumes, pea also has an exceptionally high value in organically managed farms, as their ability to form symbiotic interactions with rhizobia leads to the fixation of air-borne nitrogen [1, 4]. Besides, pea roots are colonized by arbuscular mycorrhizal fungi (AMF), which can allow the plant to access nutrients from the soil matrix more efficiently [5]. These characteristics are of tremendous use in organic and other low-input farming systems. Still, the production decreased in the past 30 years, from a peak world production of 10.5 million tons in 1992 [3]. One reason for this decline are soil-borne pathogens that can severely impact pea development and yield. The *pea root rot complex* (PRRC) can cause massive yield reductions in pea and many other legume crops [6, 7]. This complex consists of various pathogens [8], but it is assumed that iterative cropping of legumes results in an accumulation of pathogens or microbiome dysbiosis in the soil [9]. The PRRC is composed of various fungal species such as *Fusarium oxysporum* [7, 10], *Fusarium solani*, *Fusarium avenaceum* [11], *Alternaria alternata* [8], *Aphanomyces euteiches* [12] and *Rhizoctonia solani* [13], but also some bacteria species are known to cause root rot [14]. The presence of these pathogens causes root rot accompanied by wilting, damping off, and, as a consequence, substantial yield reductions [15]. Therefore, it is essential to identify approaches to maintain high yields in short crop rotation intervals [16]. Otherwise, the transition towards a more plant protein-based diet could be decelerated.

In the absence of viable management practices (besides long rotation breaks [15]), breeding has been identified as a promising solution [17]. While there have been some successes in finding partial resistances against individual pathogens such as Fusarium root rot and Didymella root rots, Rhizoctonia rot and stem rot, Pythium damping-off and Aphanomyces root rot (summarised in Wille et al. [9]), there are currently no resistant varieties available that exhibit resistance against multiple, synergistically-interacting pea pathogen complexes. Besides the above-mentioned known pathogens and beneficial taxa, many other microbial groups (such as fungi, bacteria, and oomycetes) interact with each other and the plant. These interactions can be positive, neutral, or negative for the plant [18, 19]. The knowledge of these plant-microbe interactions and how microbes affect each other in a competition scenario for carbohydrates and nutrients could be the missing puzzle piece to untangle the genetic base of PRRC. Better understanding this interlink, called the holobiont [20], can lead to diagnostic and breeding tools that improve the identification of field-relevant disease resistances. In fact, several recent studies reveal promising concepts for microbe-assisted breeding applications [21–23]. Thus, combining microbiome attributes with the diverse genetic resources of grain legumes is a key element in facilitating the breeding of high-yielding resistant pea lines [9]. Considering the microbial composition of the entire rot complex in an association panel of pea genotypes shows promise to identify robust plant quantitative trait loci (QTL) and microbial markers, which can be used in resistant pea breeding. Such QTLs can be identified in genome-wide association studies (GWAS), where phenotypes or microbial abundances are related to genetic markers in a diverse genotype panel.

This research aimed to determine the modulation capacity of pea genotypes on the root microbial composition and the heritability of individual operational taxonomic units (OTUs). It was previously highlighted that pea genotypes can modulate their root microbiota when challenged by a complex of pathogens [24]. In this study, the target questions are (i) to identify genetic interactions between the pea root microbiome and its host genetics within a diverse set of genotyped pea lines, (ii) to annotate variations in the microbial abundance to distinct genomic loci in a GWAS analysis, and (iii) to apply a subsequent regression model on the genotypes, QTLs, and microbial abundances. All three should investigate the potential of holobiont genomics for pea resistance breeding. We aligned these findings with disease phenotypes, reported by Ariza-Suarez et al. to determine a genotype - microbiome - plant phenotype connection [25].

Materials and methods

Plant material and inoculation experiment

This study utilized a subset of 252 genotypes of the 261 pea lines analysed for root rot resistance by Wille et al. [7]. The pea genotypes were grown in pots with naturally infested soil (NS) and sterilized soil (S) under controlled conditions for 21 days in a growth chamber at a 16 h/8 h

light regime with four replicates. One of the four plants was sampled for genotyping. The soil properties have been described in detail before and were characterized by a neutral ph of 7.1 and an organic matter content of 3.8%. The composition of the soil fraction was dominated by Sand (46%) and silt (37%). Plant height and shoot dry weight (SDW) were measured to assess the overall performance of the plants in the trial. The phenotypic traits of plant emergence and root-rot index (RRI: 1 = no symptoms; 6 = complete disintegration of the root system) under NS conditions, as well as the shoot dry-weight ratio between NS and S conditions ($SDW_{NS/S}$) are used to assess the overall resistance level to root rot complex [7]. Plant emergence indicates resistance against damping-off, while RRI shows resistance of plants that managed to emerge, and $SDW_{NS/S}$ indicates tolerance to disease damage [25].

Genotyping

This diverse subset of 252 genotypes from the genotype panel described before in [7] was genotyped by genotyping-by-sequencing (GBS), as described in further detail [25]. Preprocessed reads were aligned to the reference genome "Zhongwang 6" [26] using bowtie2 [27], and SNPs were called using NGSEP (v4.1.0 [28]). Genotype calls with a minimum quality of 30 were filtered out. Similarly, sequence variants with a minor allele frequency (MAF) below 0.02 and a maximum heterozygosity rate of 0.05 were filtered out. Sequence variants with more than 78% missing calls were also removed to reduce the proportion of missing data in the entire genotypic matrix to approximately 30%. A total of 18,267 markers evenly distributed across all seven chromosomes were used to perform a genome-wide association study (GWAS) and genomic prediction (GP). Missing genotyping information was imputed using *beagle* (v22.46e [29]), with default parameters for the genomic prediction, while no imputation was performed for the GWAS analysis.

Microbiome characterization

Pea root systems were sampled after 21 days, as described in Wille et al. [7] and Gfeller et al. [24]. In short, roots were shaken to remove loosely attached soil and washed in sterilized water. After lyophilization and milling, DNA was extracted from 15 mg dried root powder using the Mag-Bind Plant DNA DS 96 Kit (Omega Bio-Tek, Norcross, United States) following the manufacturer's instructions.

Microbiota profiling was performed as previously described [24]. For fungal communities, the entire ITS region was amplified using the ITS1f/ITS4 primers and sequenced by the Genome Quebec Innovation Center (Montreal, Canada) using a PacBio (Sequel II) sequencer. Quality filtered amplicons were error-corrected to obtain zero radius operational taxonomic units (zOTUs) using UNOISE [30]. zOTUs were further clustered into OTUs of 97% nucleotide similarity with UPARSE [31]. The UNITE (V83 [32]), ITS reference database was used to predict taxonomic associations. For the profiling of the bacterial communities, the V3 and V4 hypervariable regions of the 16 S rRNA gene were amplified using the V3F and 799R primers. Amplicons were sequenced on an Illumina MiSeq sequencer by the Genome Quebec Innovation Center (Montreal, Canada). The bioinformatic analysis was done in QIIME2 [33] where the DADA2 pipeline [34] was used for amplicon sequence variants (ASV) calling and before clustering into OTUs of 97% nucleotide similarity (vsearch [35]). Taxonomy was assigned using the SILVA database [36]. An additional taxonomic classification was performed by a local *blastn* [37] mapping of OTU sequences to the entire NCBI fungi and bacteria database of complete genomes (downloaded 22.03.2023 [38]). As the UNITE classification did not provide a sufficient resolution down to genus or species level for most OTUs, we decided to add this BLAST step, being aware of its limitations and uncertainties. A maximum of 10 matches was reported for each OTU in the mapping process, from which the best match observed was used to estimate a "best guess" of the OTU's species. If different taxa appear within the same taxonomic rank (e.g. species), the next higher rank was chosen (e.g. genus).The identity threshold was set to 95% for fungi and 90% for bacteria, with a minimum alignment length of 300 bp.

Statistical analysis on the microbiota profiling data was performed as previously described [24]. In short, the alpha diversity indices OTU richness and Shannon Index were calculated on rarefied count tables. Microbial community compositions (beta diversity) were visualized by Principal Coordinates Analysis (PCoA) on Bray-Curtis dissimilarity matrixes. Differential abundance analysis of individual OTUs was performed using the ALDEx2 pipeline [39] on emergence and RRI as a resistance trait for fungi and bacteria. An OTU was considered differentially abundant when the association with the two resistance traits was significant ($p < 0.05$ after correction for multiple testing). Ultimately, four classes were specified – differential abundant bacterial OTUs (da bOTU), differential abundant fungal OTUs (da fOTU), as well as not resistance-associated OTUs for both bacteria (bOTU) and fungi (fOTU). CLR transformed count tables obtained through the ALDEx2 pipeline were used as an abundance score for all analyses in thispaper.

Genotype-microbiome relationship approximation by PCA

Two principal component analyses (PCA) were performed to estimate genotype relationships. The first was based on the genotype of each pea line, considering all

available 18,267 markers. The second was constructed based on the OTU-abundance scores for each pea line. All 1,227 fungal and bacterial OTUs were included in a second PCA. OTUs and markers with the highest effect on plant health status were identified using both PCA. A clustering of resistant pea lines was performed on both genotype and OTU-based PCAs to identify an intersection between the (i) OTU and (ii) marker-derived genotype PCA positions. Each genotype's position was scaled against the center of the worst class (class 6). The scaling was performed across the first 5 PCs (which explain the majority of the variation), corrected by the explained variance of each PC. The value obtained for each PC was summed up for each genotype to obtain a "distance value" from the center of the highest susceptibility class six. The 90% quantile of the most distant genotypes was calculated to extract the genotype with the greatest distance to the others for both approaches (OTU abundance and plant genetic). Similarities between these classes were defined by the ratio of matched to unmatched genotypes. We hypothesized that a high number of matches between these two groups would indicate an effect of pea genotype on OTU abundance and microbiome composition. Additionally, Mantel's test was employed to analyze the correlation between pea genotype genomic distances and associated microbiome distances, which were based on the first five principal components (PCs). The analysis utilized the mantel function from the R package vegan with 999 permutations to assess these relationships. To minimize the impact of outliers, Spearman's correlation analyses were employed [40, 41].

Genome-wide association study

A genome-wide association study was performed using the *R* package *rrBLUP* (version 4.6.2 [42]), to assess the genomic background of OTU abundance. We included five principal components of the pea genotype-based PCA and the kinship matrix for all markers with an MAF > 0.03 to correct for population structure.

In the first run, we performed a GWAS for the alpha and beta diversity of the entire microbiome. OTU richness and Shannon Index were taken as proxies of alpha diversity. The first two principal coordinates of the microbiome ordination were used for beta diversity, as described elsewhere [43]. We estimated narrow sense genomic heritability using an additive covariance matrix in the *sommer* package function *mmer* with 1,000 iterations for alpha and beta diversity.

In a second run, we performed a GWAS on all 1,227 OTUs separately. To do this, we clustered the OTUs into four different groups - "da bOTU", "da fOTU"," bOTU", and "fOTU". Each group contained 34, 51, 861, and 366 units, respectively. We applied a Bonferroni corrected p-value threshold of 0.05 for each of these four classes to account for type I errors. Therefore, we used the formula:

$$p_{critical} = \frac{0.05}{\sum Markers * \sum OTUs_n^m} * 0.9$$

to account for the multiple testing problem arising from the number of markers and multiple OTUs from group *n* with size *m*. We relaxed the threshold marginally by a factor of 0.9 to account for linkage blocks in the genotypes studied.

Analogous to the alpha and beta diversity, the narrow sense heritability was calculated for each OTU. Furthermore, we included the QTLs identified for the plant phenotypes in Ariza-Suarez et al. [25] to distinguish potential co-segregations of OTU and plant phenotype QTL.

Prediction of pea phenotypes using pea genomic markers and OTU abundance in a holobiont approach

Genomic prediction (GP) was performed to predict the (i) emergence rate and the (ii) root rot index by fitting Bayesian models (Bayes A, Bayes B). We used the R package BGLR (v1.1.0 [44]), with 6,000 iterations and 1,000 as burn-in. Five-fold cross validations in ten replications were performed so that each genotype was used once for the model validation (Test set size = 50 genotypes). The Bayes-B model was used solely for the GP based on all markers, as it has already been identified by Ariza-Suarez et al. [25] that few QTL loci have a major effect on the phenotypic variation in the tested population of pea lines. We used Bayes-A for all other GPs, assuming all predictors have at least a small effect on seedling emergence and root rot index. In both Bayes models, the leaf morphology (leafless, semi-leafless) was added as a fixed cofactor due to its agronomic value. Eighteen different predictor combinations and compositions were tested, as listed below:

- Plant genomic marker-based

  1. All available markers
  2. QTL markers identified for plant resistance traits (e.g. RRI, germination rate)
  3. QTLs for both plant traits and OTU abundance together
  4. The two most significant QTLs from the OTU GWAS
  5. QTLs identified for non-differentially abundant OTUs (both fungi and bacteria)
  6. QTLs identified for differentially abundant OTUs (both fungi and bacteria)

- Additionally, as the explained variance of all OTU-associated QTLs was always smaller 1, we

repeated the genomic regression approach using the abundance of different OTU sets instead of the marker's information. The abundance of:

7. all OTUs
8. all heritable OTUs
9. PCA derived OTUs (from Fig. 1)
10. PCA & QTL derived OTUs
11. The most descriptive OTUs

We collected the information on the three most dominant OTUs by running a genomic regression model using all PCA derived OTUs. Across all cross validations (CV), the top 50% OTUs with the highest "marker effect" in the model were collected. The OTU intersect within the 10 CV was determined to find the most descriptive OTUs. Afterward, the genomic regression model was repeated with only these three OTUs.

– Lastly, the combination of genomic markers and OTU abundance.

12. all QTLs and all OTUs
13. all markers and all OTUs
14. the two most significant QTLs, together with the most descriptive OTUs

was assessed. The estimated phenotype per predictor combination was extracted from the model and compared by Pearson's correlation coefficient to the measured phenotype to obtain a "prediction ability".

Results

Plant genotype and OTU abundance co-cluster with respect to plant disease phenotype

We were first interested in testing whether a general correlation exists between microbial abundance and pea genotypes. We, therefore, performed separate PCAs for the microbial abundance (OTUs) and the pea genotypes. The first five PCs highlighted a significant correlation between the OTU abundance and the pea genotypes ($p = 0.01$).

Based on bOTU and fOTU abundance levels for each pea genotype, the first and second principal components of the PCA explained 12% of the total variance. The first five PCs explained 20% of the variation. The visualization of the first two PCs revealed a continuous shift of the phenotype's susceptibility scores towards the left, lower, and upper right edges (Fig. 1A). While genotypes clustering in the upper right quadrant were associated with high infection rates, genotypes in the far left and bottom areas indicated low infection with the pea root rot complex (PRRC). An analog PCA based on the pea genomic markers revealed a comparable rate of explained variance (Fig. 1B). While a considerable portion of high and low susceptible genotypes do not differentiate in the center, another set of resistant genotypes is clustered at the left (diamond) and bottom right (hexagon) ends of the distribution (Fig. 1B). Interestingly, the clustering of the low-susceptibility genotypes S30, S49, S166, S62, S71, S10, and S98 (hexagon) was identical in the OTU- and genotype-derived PCAs, forming one group (Fig. 1A/B). The four most descriptive OTUs in this cluster were fOTU285, fOTU782, fOTU1657, and fOTU1508 (Suppl. Table 2). With descriptive, we refer to the OTUs with the highest PC loadings across the top two PCs. A BLAST search indicated these fOTUs belong to the family *Chaetomiaceae* (fOTU285) and the genus *Dactylonectria* (fOTU782, fOTU1657, and fOTU1508). The second group of genotypes (diamond) with low susceptibility consists of the nine genotypes G7, G17, G18, G20, G25, G34, G43, and G88. The most descriptive OTUs for this genotype cluster are bOTU121, bOTU115, bOTU107, bOTU191, and bOTU144. In contrast to the other low-susceptibility clusters, all originate from the bacterial kingdom, and none are differentially abundant. These bOTUs are related to *Clostridium* sp. (bOTU121, bOTU115), *Aminipila* sp. (bOTU191), and *Pelosinus* sp. (bOTU144).

The most descriptive OTUs for the high susceptibility cluster are bOTU63, bOTU28, fOTU53, and bOTU26. According to the best BLAST search match, these are related to *Serratia sp*, *Stenotrophomonas sp.* genus, or *Tuber melanosporum*. Except for bOTU63, all are da bOTUs. In general, the 20 most descriptive OTUs forming this cluster of susceptible genotypes originate in the kingdoms of fungi (5) and bacteria (15) kingdoms (Suppl. Table 2). Besides the count bias, the PCA indicated that bacteria had a higher explanatory power for the cluster of highly infected pea genotypes than fungi. In contrast, the two low-susceptibility groups were described by a significant effect of either fungi (19 out of 20 for the left-tailed group in Fig. 1A, Suppl. Table 2) or bacteria (11/20 for the top-tailed group in Fig. 1A, Suppl. Table 2).

GWAS of microbiome abundance co-locate with previous and reveal new resistance QTLs

With initial evidence of genotype-microbiome co-linearity, we aimed to attribute these relations to genomic loci in a GWAS. We first examined the alpha and beta diversity of the entire microbial community (Fig. 2). Beta diversity revealed two significant loci for fOTUs, both located on chromosome 6, region 85 MB-95 MB and region 264 MB. The same loci showed an association in the second PCoA for bacterial beta diversity. However, the critical -logP threshold was not exceeded, and the genomic heritability of beta diversity ranged from 0.14 to 0.28, while going up to 0.82 in the fungi beta diversity.

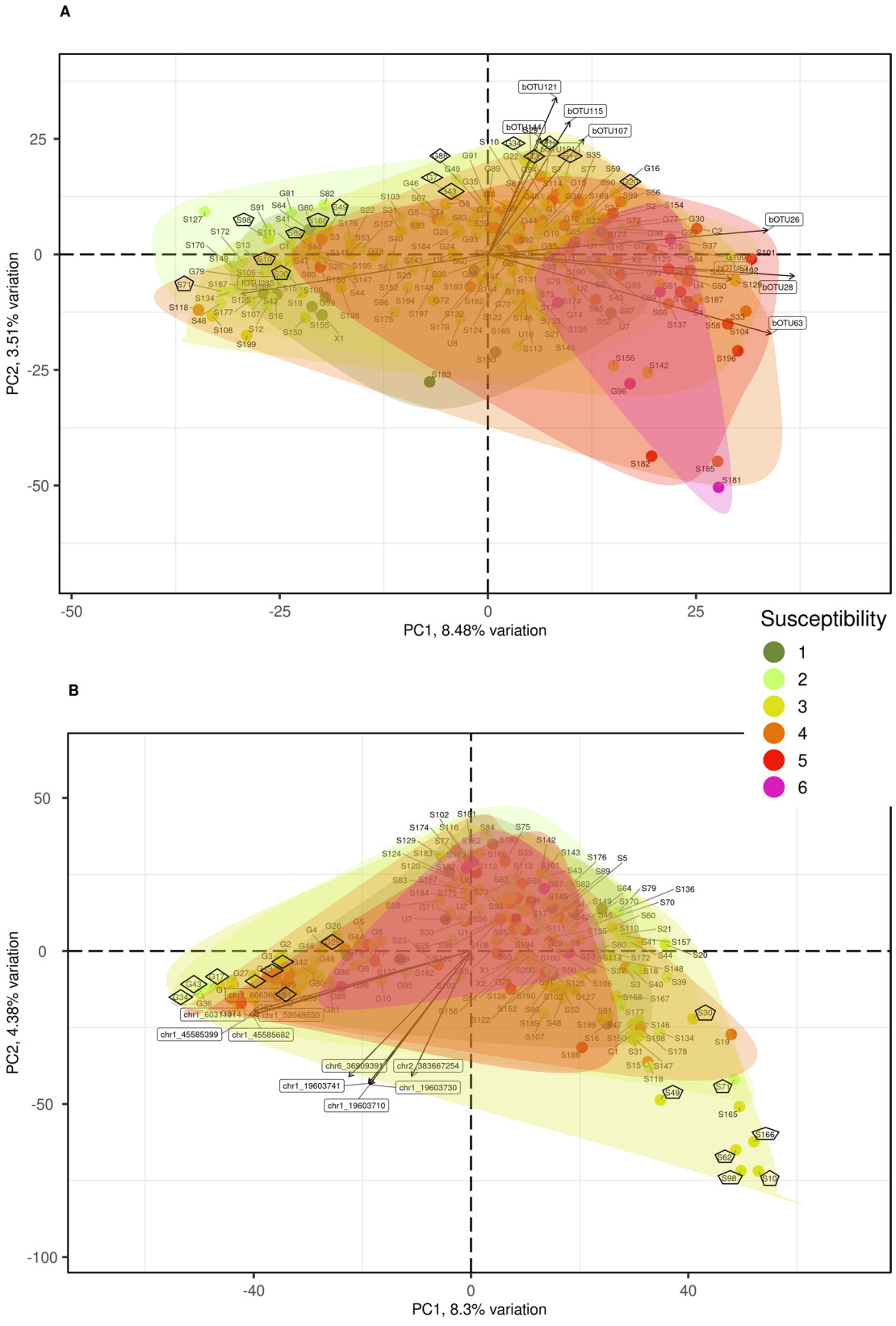

Fig. 1 (See legend on next page.)

(See figure on previous page.)

Fig. 1 First and second principal component analysis of the plant genotype relationships based on (**A**) the microbial abundance of both fungi and bacteria combined and (**B**) on 17,896 genomic markers. Each dot represents one of 252 plant genotypes, colored by the observed phenotypic susceptibility to root rot. A root rot index (RRI) of 1 indicates low infection, while a value of 6 represents the most infected genotypes. The colored areas show clusters of similar susceptible genotypes. Arrows highlight the most relevant loading in the first and second component (**A** – OTU; **B** - Marker). If loadings overlap, only the most relevant one is presented. The hexagon and rhombus illustrate two groups of resistant genotypes, which keep their composition and distance in microbial (**A**) and genomic marker (**B**) based PCAs

In the next step, we investigated whether genome-wide associations exist for the abundance of individual OTUs. The GWAS of differentially abundant (da) OTUs revealed 143 highly significant markers at 54 independent loci across all seven chromosomes. Twenty of these loci are associated with more than one OTU, while only four are linked to both fungi and bacteria (Figs. 3A/B and 4). The major region observed is located on chromosome 6 from 85 to 95 MB and consists of 10 individual QTLs (Fig. 3A.2). Forty-seven fungal and three bacterial OTUs were found to be associated with this region. Additionally, two multi-bOTU loci (with >3 OTUs associated) were found on chromosome 1 at positions 157–161 MB, chromosome 2 at position 408 MB, and chromosome 6 at position 316 MB.

In total, we found significantly associated markers for 98 different OTUs, of which 39 were identified as bOTUs (5% of all bOTUs observed in the root), 11 in the group of da bOTUs (32% of all da bOTUs), 23 for fOTUs (6%), and 25 for da fOTUs (49%). We found 57 associated markers at ten independent loci for all daOTUs. QTLs on chromosome 6, position 85–95 MB, co-segregated with QTLs for shoot dry weight ratio, root rot, and seedling emergence identified by Ariza-Suarez et al. [25] (Fig. 3B). The notable aspect of this co-segregation is that the OTU-QTL marker associations are much stronger than pea resistance QTL associations (higher LOD score Fig. 4).

Next, we examined the genomic heritability (h^2) for all operational taxonomic units (OTUs). Some differentially abundant OTUs exhibited a heritability of up to $h^2 = 0.46$, while individual OTUs reached as high as 0.99 when factoring in all OTUs found in the pea root (Fig. 3C). Among the 1,227 OTUs studied, 377 displayed a heritability of 0, and the average genomic heritability was measured at 0.059, with a standard deviation of 0.09. Heritabilities were lowest for non-daOTU.

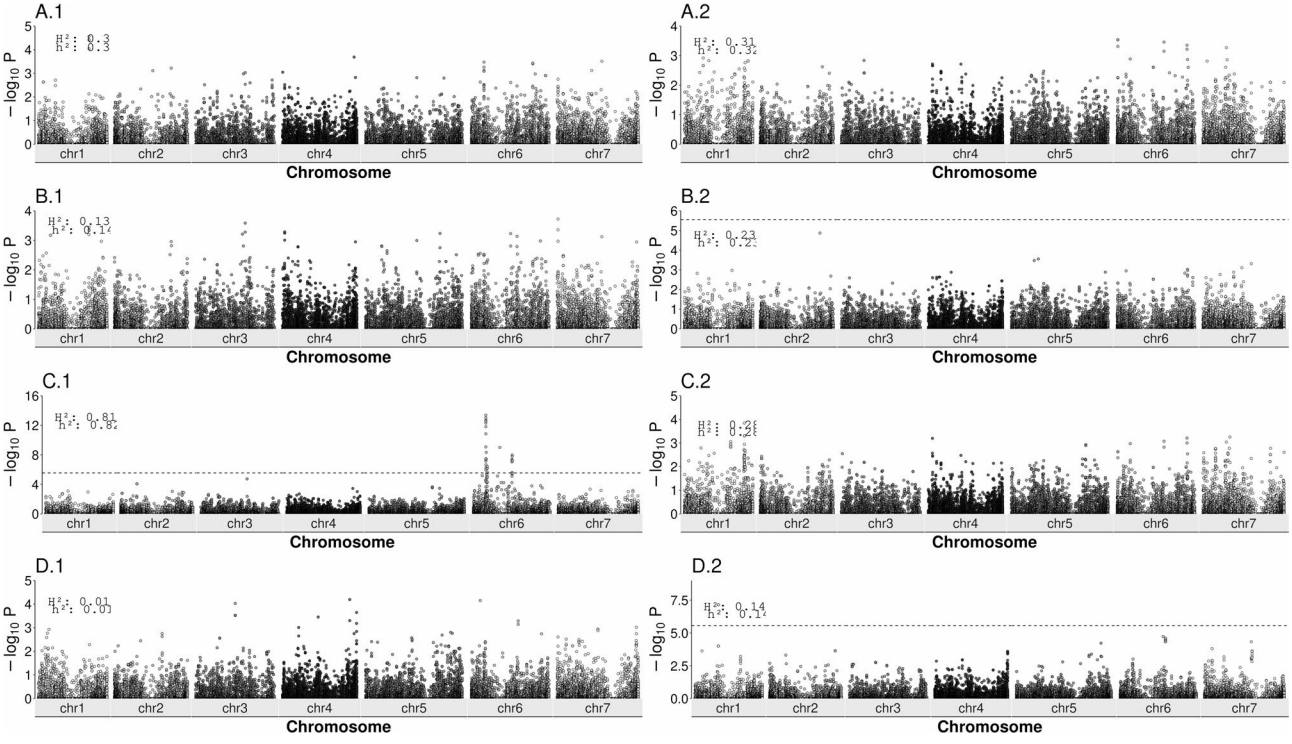

Fig. 2 Manhattan plots of the root microbiomes' alpha and beta diversity. Alpha diversity (Shannon index and richness) was tested for associations with genomic loci in a GWAS (Subfigures A & B). The first and second principal coordinate of an ordination plot were used to approximate beta diversity (Subfigures C & D). The analyses were performed separately for fungi (left, **A.1** – **D.1**) and bacteria (right **A.2** – **D-2**). Horizontal dashed lines indicate the minimum threshold of significance after multiple testing corrections. Genomic broad-sense (H^2) and narrow-sense (h^2) heritability were calculated for each and illustrated in the top left corner. No dashed lines imply no detected QTLs

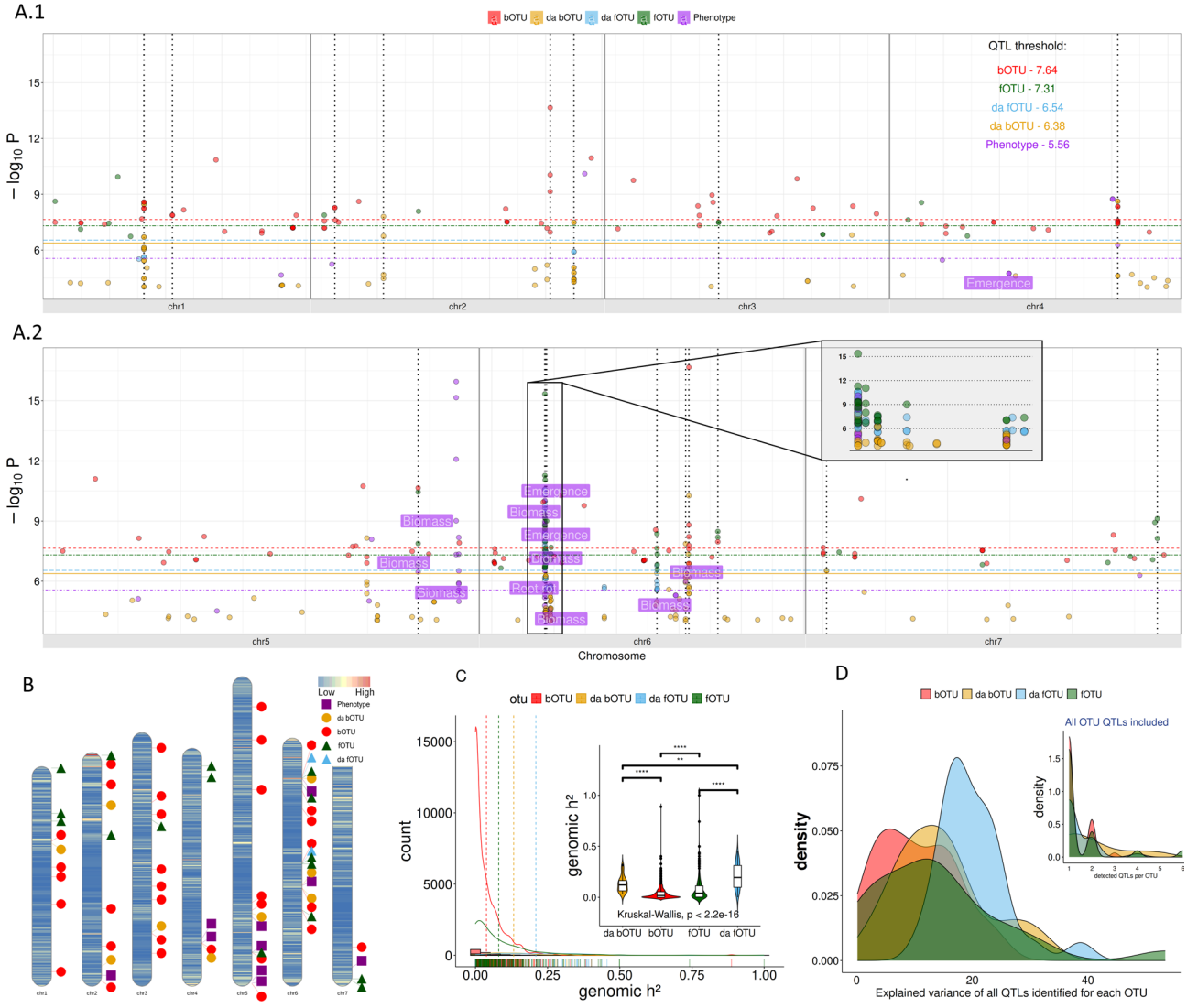

Fig. 3 All QTLs of all single OTU GWAS compiled in one figure. **A** a summary plot of all detected genomic loci. Horizontal lines indicate the multiple-testing corrected threshold for each category – adjusted by marker and tested feature (OTU, phenotype) count. Vertical dashed lines indicate robust QTLs. The QTLs related to root rot, emergence, or shoot dry weight ratio are annotated with trait names. The region with the most QTLs was zoomed in to illustrate sub-QTLs. **B** overview of marker density and QTL locations. **C** the summary figure of heritability (da [differential abundant], non-da [not differential abundant]). Vertical lines indicate the average genomic heritability within the four groups. The boxplot (subplot) highlights the statistical comparison of the four groups. **D** Histogram of QTLs explained variance (da, non-da). The colors represent the four traits groups bOTU (all bacterial OTUs classified, red), fOTU (all fungal OTUs classified, green), da bOTU (differential abundant bacterial OTUs, yellow), da fOTU (differential abundant fungal OTUs). The subplot illustrated how many QTLs per OTU were detected

groups, with an average h^2 of 0.04 for bOTUs and 0.1 for fOTUs, respectively. The genomic heritabilities for the da bOTU and da fOTU groups were 3.25 times higher ($p < 10–15$, Wilcox test) and 2.1 times higher ($p < 10-7$), with values of 0.13 and 0.21, respectively. The average genomic heritability of QTL-associated OTUs was 0.156, significantly higher ($p < 0.001$) than that of the non-QTL-associated OTUs (h^2=0.048).

In addition, we examined the heritability of the 60 most prominent OTUs identified in the prior PCA analysis. These OTUs, which differentiate PRRC (daOTUs), showed a significantly higher heritability of h2 = 0.176 compared to h2 = 0.05 for all observed OTUs ($p < 0.001$ – as determined by the Kruskal-Wallis rank sum test). Among these 60 OTUs, 21 were significantly associated with QTLs in the pea genome. In total, we identified 36 QTLs across three distinct loci for these 21 OTUs. All but one locus were located on chromosome 6, with the most significant markers [27] located within the 85–95 MB window. Notably, the majority of the 36 significant markers were associated with the left-tailed positive class (PCA of OTU abundance), connected with fOTUs (Fig. 1A).

	core QTL interval		Count of QTLs		-logP score		MAF	
Chromosome	Start	End	Fungi	Bacteria	Min	Max	Min	Max
Chr - 1	**157,658,746**	**161,258,611**	**0**	**9**	**6.70**	**8.58**	**0.103**	**0.125**
Chr - 1	211,956,107	211,956,108	0	2	7.87	7.87	0.118	0.118
Chr - 2	24,347,359	24,347,383	0	2	8.28	8.28	0.047	0.047
Chr - 2	110,978,990	110,978,990	0	2	6.75	7.80	0.051	0.051
Chr - 2	**408,029,956**	**408,029,956**	**0**	**3**	**9.15**	**13.66**	**0.041**	**0.041**
Chr - 2	450,369,814	450,369,844	0	2	7.49	7.49	0.090	0.090
Chr - 3	147,341,198	149,843,028	0	2	7.86	8.37	0.080	0.082
Chr - 3	172,407,825	174,335,788	0	2	8.57	8.96	0.044	0.056
Chr - 3	184,191,113	184,191,129	2	0	7.49	7.49	0.043	0.043
Chr - 3	421,525,699	423,340,692	0	2	6.81	8.36	0.043	0.047
Chr - 4	**410,554,822**	**410,554,825**	**0**	**4**	**8.34**	**8.62**	**0.097**	**0.097**
Chr - 5	476,104,141	481,246,025	0	2	7.73	7.75	0.074	0.081
Chr - 5	581,088,213	581,088,213	2	1	7.88	10.65	0.048	0.048
Chr - 6	**85,080,320**	**94,899,726**	**47**	**3**	**6.66**	**15.34**	**0.048**	**0.287**
Chr - 6	262,697,473	264,763,074	3	1	6.78	8.56	0.046	0.083
Chr - 6	310,779,718	314,941,098	0	3	6.40	7.87	0.062	0.108
Chr - 6	**315,947,701**	**315,947,760**	**0**	**7**	**6.72**	**16.67**	**0.054**	**0.061**
Chr - 6	362,444,984	362,444,984	2	1	7.96	8.48	0.045	0.045
Chr - 7	5,931,102	5,931,171	0	2	6.52	6.52	0.068	0.068
Chr - 7	536,300,839	536,300,839	2	0	8.14	9.12	0.074	0.074

Fig. 4 List of all detected QTLs with more than two OTUs mapping to the same locus. Information on the genomic locus, the QTL interval, the number of QTLs detected for fungi and bacteria for each QTL interval, the corresponding minimum and maximum -logP values, and the minor allele frequency (MAF) of each QTL is provided. Loci with more than two associated OTUs are highlighted in black rows

Finally, we assessed the proportion of OTU abundance variance attributable to the detected QTLs (Fig. 3D). On average, these markers accounted for approximately 14.3% of the total variance. For most OTUs, only a single QTL was observed. The QTL explained, on average, 9.87% of the total variance. The highest average explained variance was observed for the group of da fOTUs (20.15%), followed by the differentially abundant bacterial OTUs (14.71%). The explained variation reached up to 53% for single OTUs (Fig 5). In general, the explained variance of all fOTU QTLs and bOTU QTLs was not significantly different.

Heritable associations between OTU abundance and disease resistance

The relative abundance of several OTUs was strongly correlated with root rot index and plant emergence (Fig. 5). A total of 47 OTUs (30 fOTUs and 17 bOTUs) showed a QTL's explained variance above 15%.

Fungi

A total of five fOTUs were identified by a QTL with an explained variance exceeding 30% (fOTU285, fOTU1517, fOTU782, fOTU1255, bOTU12). For the highly heritable fOTU285 and fOTU782 (h^2>0.4; Fig. 5), we identified four and six QTLs that account for 32% and 53% of the total variance in abundance, respectively, alongside 13% and 12% of the variance in the root rot index, and 20% and 29% of the variance in seedling emergence for each fOTU. Both fOTUs have a significant negative and positive correlation with root rot and seedling emergence, respectively, and were most abundant in one of the PCA 'resistant' groups (Fig. 1), indicating a positive effect of these OTUs on the plant's health status. The best BLAST

		BLAST		Heritability	Explained variance of QTLs on [%]			Correlation r		Estimated effect on	QTL for the corresponding OTU		
Abundance	OTU	best guess	Class	h^2	OTUs	Root rot	Emergence	Root rot	Emergence	Root rot	QTLs (most significant per LD interval)	QTL level	Count sig. markers
fOTU	fOTU793	Fusarium oxysporum	unkown	0.499	28.37	11.95	22.35	0.319	-0.536	negative	chr6_85,084,236	9.18	2
fOTU	**fOTU285**	**Chaetomiaceae sp.**	**Sordariomycetes**	**0.499**	**31.19**	**13.37**	**19.84**	**-0.243**	**0.549**	moderate positive	**chr6_85,080,347; chr6_264,762,995; chr6_265,223,271**	**7.35-11.27**	4
da fOTU	**fOTU1517**	**Dactylonectria estremocensis**	**Sordariomycetes**	**0.456**	**38.70**	**7.49**	**20.44**	**-0.356**	**0.639**	positive	**chr6_85,085,481**	**9.97**	2
da fOTU	fOTU180	Fusarium cf.	unkown	0.436	26.87	13.60	20.44	0.340	-0.521	negative	chr6_85,080,347	9.46	2
fOTU	**fOTU782**	**Dactylonectria estremocensis**	**unkown**	**0.436**	**53.39**	**11.81**	**20.44**	**-0.254**	**0.566**	moderate positive	**chr6_85,080,320; chr6_95,117,472; chr6_264,763,074**	**7.64-15.34**	6
fOTU	fOTU156	Chaetomium globosum	unkown	0.426	20.31	7.02	24.55	0.167	-0.316	moderate negative	chr6_85,085,481	8.61	1
da fOTU	fOTU780	Fusarium keratoplasticum	unkown	0.393	16.51	12.38	17.94	0.275	-0.618	moderate negative	chr6_85,080,347	7.02	1
da fOTU	fOTU712	Fusarium keratoplasticum	unkown	0.390	17.25	12.38	17.94	0.264	-0.637	moderate negative	chr6_85,080,347	7.63	1
da fOTU	fOTU1487	Fusarium vanettenii	unkown	0.386	16.84	12.38	17.94	0.244	-0.624	moderate negative	chr6_85,080,347	7.35	1
da fOTU	fOTU856	Golubevia sp.	Sordariomycetes	0.384	25.28	13.60	20.44	0.358	-0.526	negative	chr6_85,080,347	10.31	2
fOTU	fOTU945	Fusarium vanettenii	Sordariomycetes	0.379	24.32	13.60	20.44	0.342	-0.562	negative	chr6_85,080,347	9.34	2
fOTU	fOTU272	Chaetomium sp.	Sordariomycetes	0.363	21.31	7.02	24.55	0.122	-0.338	moderate negative	chr6_85,085,481	9.26	1
da fOTU	**fOTU1255**	**Dactylonectria estremocensis**	**Sordariomycetes**	**0.362**	**30.43**	**7.02**	**7.34**	**-0.336**	**0.590**	positive	**chr6_85,085,481**	**10.54**	1
da fOTU	fOTU150	Dactylonectria estremocensis	Sordariomycetes	0.354	29.07	12.38	17.94	-0.285	0.604	moderate positive	chr6_85,080,347	8.34	1
da fOTU	fOTU1557	Dactylonectria sp.	Sordariomycetes	0.352	25.06	11.76	21.35	-0.349	0.624	positive	chr6_85,080,362; chr6_264,762,847	6.78-9.77	2
da fOTU	fOTU860	Fusarium vanettenii	Sordariomycetes	0.352	16.13	12.38	17.94	0.345	-0.609	negative	chr6_85,080,347	8.39	1
da fOTU	fOTU1292	Clonostachys rosea	Sordariomycetes	0.351	16.02	10.55	20.12	-0.199	0.555	moderate positive	chr6_85,080,362	7.5	1
da fOTU	fOTU290	Thelonectria olida	Sordariomycetes	0.312	22.32	12.38	17.94	-0.302	0.579	positive	chr6_85,080,347	8.47	1
da fOTU	fOTU312	Dactylonectria sp.	unkown	0.312	15.97	12.38	17.94	-0.247	0.485	moderate positive	chr6_85,080,347	7.3	1
da bOTU	bOTU26	Stenotrophomonas sp.	Gammaproteobacteria	0.307	15.58	12.38	17.94	0.342	-0.561	negative	chr6_85,080,347	8.6	1
da fOTU	fOTU294	Ilyonectria destructans	Sordariomycetes	0.304	19.63	10.55	20.12	-0.330	0.550	positive	chr6_85,080,362	8.01	1
da fOTU	fOTU1508	Dactylonectria sp.	Sordariomycetes	0.286	19.99	12.38	17.94	-0.374	0.605	positive	chr6_85,080,347	9.46	1
da fOTU	fOTU1284	Fusarium vanettenii	Sordariomycetes	0.273	21.37	12.38	17.94	0.365	-0.542	negative	chr6_85,080,373	10.59	1
da bOTU	bOTU69	Flavobacterium oreochromis	Bacteroidia	0.269	25.48	3.80	4.40	-0.173	0.368	moderate positive	chr1_161,258,593; chr6_314,941,098	7.35-8.47	3
da fOTU	fOTU256	Dactylonectria estremocensis	unkown	0.257	17.83	10.55	22.28	-0.210	0.581	moderate positive	chr6_85,080,362	7.78	2
da fOTU	fOTU20	Orbilia oligospora	unkown	0.228	22.83	12.38	17.94	0.344	-0.597	negative	chr6_85,080,347	9.63	1
da fOTU	fOTU287	Dactylonectria estremocensis	Sordariomycetes	0.224	16.55	7.96	18.09	-0.214	0.512	moderate positive	chr6_85,084,236	7.95	1
da fOTU	fOTU1436	Fusarium cf.	unkown	0.214	15.77	12.38	17.94	0.304	-0.419	negative	chr6_85,080,373	7.57	1
da fOTU	fOTU296	Microdochium nivale	unkown	0.181	23.83	12.74	22.71	-0.281	0.579	moderate positive	chr6_85,080,362	8.02	4
fOTU	fOTU789	Dactylonectria estremocensis	Sordariomycetes	0.175	15.29	12.38	17.94	-0.274	0.409	moderate positive	chr6_85,080,347	8.76	1
da fOTU	fOTU280	Dactylonectria estremocensis	Sordariomycetes	0.154	19.03	11.45	20.83	-0.204	0.522	moderate positive	chr6_85,080,362	6.67	2
bOTU	bOTU1404	Sorangium cellulosum	Polyangia	0.151	22.32	0.68	0.95	0.070	-0.055	neutral	chr6_110,804,241	10.27	1
da bOTU	bOTU28	Stenotrophomonas sp.	Gammaproteobacteria	0.123	17.38	12.38	17.94	0.430	-0.437	negative	chr6_85,080,373	7.6	1
da bOTU	bOTU47	Niastella koreensis	Bacteroidia	0.120	17.52	2.08	6.93	-0.339	0.312	positive	chr6_310,779,718; chr6_315,947,701	6.87-7.87	2
da bOTU	**bOTU12**	**UNVERIFIED_ORG: Kinneretia**	**Gammaproteobacteria**	**0.117**	**30.74**	**0.14**	**7.77**	**-0.400**	**0.295**	positive	**chr1_161,258,593; chr2_110,978,990; chr5_498,784,941; chr6_315,947,701**	**6.7-10.26**	5
fOTU	fOTU538	Lasiosphaeriaceae sp.	Sordariomycetes	0.100	19.05	0.44	3.64	-0.039	-0.134	neutral	chr2_173,516,613	8.08	1
bOTU	bOTU423	Paenibacillus xylanilyticus	Bacilli	0.063	17.04	0.05	0.54	-0.041	-0.023	neutral	chr7_61,249,824	10.11	1
bOTU	bOTU51	Sphingomonas psychrotolerans	Alphaproteobacteria	0.042	23.38	2.12	2.96	-0.098	0.203	neutral	chr1_161,258,593	8.24	2
bOTU	bOTU608	Chitinophaga sp.	Bacteroidia	0.026	15.36	1.18	2.64	-0.148	-0.010	moderate positive	chr5_481,246,025; chr6_362,444,984	7.75-7.96	2
bOTU	bOTU606	Legionella pneumophila	Gammaproteobacteria	0.002	24.80	0.57	1.81	0.054	-0.120	neutral	chr2_408,029,956	10.04	1

Fig. 5 Summary of OTUs characterized by an explained variance above 15% (using the detected QTL(s) to calculate the explainable variance for each OTU). Besides the abundance class (da, not da; da = differential abundant), the nearest blast species candidate (best guess) and the identified class by the UNITE reference alignment (Class) are illustrated to characterize the OTU. Further, the genomic heritability, the detected QTLs, and their explanatory power on the variance of the OTU abundance as well as root rot and emergence, are presented. Besides, the correlation of the OTU's abundance towards the plant phenotypes emergence and root rot is also illustrated. Black-colored rows highlight OTUs, where QTLs could explain more than 30% of the total OTU abundance variance

estimates for these two OTUs were *Chaetomiaceae sp.* and *Dactylonectria sp. Dactylonectria* was the most frequently observed genus in the group of these 40 most genetically heritable OTUs with 11 occurrences (Fig. 5). A positive or moderately positive effect on the root rot index of the pea lines could be attributed to all 11 (Fig. 6). We also found nine of these 40 OTUs belonging to the genus *Fusarium*. They all had either moderately negative or negative effects on pea root rot.

Bacteria

A single bOTU was described by a QTL with more than 30% explained variance (bOTU12). In contrast to fungi, equal numbers of QTLs were found for non-differentially and differential abundant bacterial OTUs (Fig. 6). The genomic heritability of these bOTUs was similar to fungi, with the highest genomic heritability observed for bOTU26 (0.31) and bOTU28 (0.12). These two daOTUs could be annotated to the genus *Stenotrophomonas sp*, with a single common QTL on chromosome 6, position 85 MB (bOTU26, bOTU28). Negative effects on the pea phenotypes can be reported for this genus. Together with bOTU63, these four had the largest effects on the PCA cluster of highly susceptible pea genotypes (Fig. 1). bOTU63, identified as *Serratia sp.*, did not indicate a significant QTL (Max. marker association -logP = 5.5 @ chr6, 85 MB), but was characterized by a genomic heritability of h^2=0.16.

Genomic prediction of plant health by OTUs and QTLs

After significant associations to single plant genomic markers were detected for the presence or abundance of fungal and bacterial OTUs, we aimed to utilize significant SNP markers in a genomic regression approach to predict the pea root rot and emergence phenotypes. For comparative reasons, we also utilized all QTLs detected for all OTUs and plant phenotypes affected by the root rot complex (root rot index, shoot dry weight ratio, emergence rate).

Root rot

The evaluation of these genomic regression models revealed a significantly higher prediction accuracy for those approaches where OTU markers (OTU abundance) were used alone or combined with genomic markers ($\mu = 0.53$) to predict the pea root rot score compared to genomic markers alone ($\mu = 0.27$; Fig. 7). The lowest prediction ability was obtained when all available genomic markers were used (average $r^2 = 0.09 \pm 0.12$). In the analysis of plant genomic QTLs, the model utilizing 16 resistance phenotype QTL markers demonstrated the greatest average predictive ability ($r^2 = 0.36 \pm 0.09$), outperforming all other genomic marker combinations incorporating OTU-derived QTL markers (0.29 ± 0.09). OTU markers (based on OTU abundances) significantly increase prediction ability up to an average of $r^2 = 0.59 \pm 0.09$ across five cross-validations and ten replications (best result obtained for heritable OTUs). The average prediction ability remained similar when removing all nonheritable OTUs (all OTUs

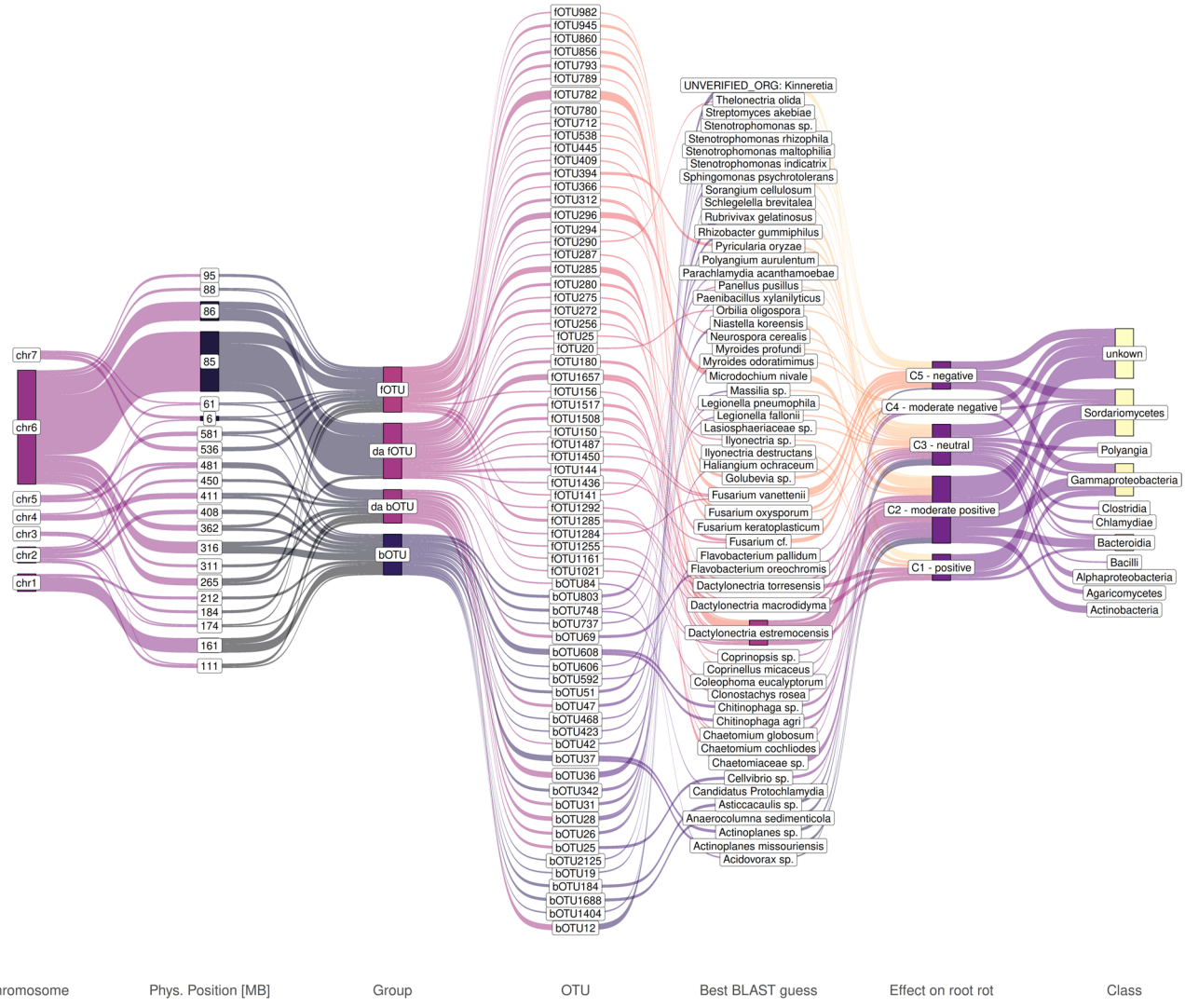

Fig. 6 Sankey plot illustrates the interconnection of QTL loci, OTUs, their most similar blast guess, and their relation to the plant phenotype root rot. Lines connect each OTU with genomic features, pea phenotypes and genus and class information. The thickness of the line presents the abundance of observations. OTUs are linked to QTL regions and are clustered in taxa, determined by BLASTing. Grouping in class C1 to C5 for the effect on root rot is based on the correlation of the OTU abundance and the root rot index C1 = correlation $r < -0.3$; C2 – $-0.3 < r < -0.1$; C3 – $-0.1 < r < 0.1$; C4–$0.1 < r < 0.3$; C5 – $r > 0.3$. C1 – positive indicates a low OTU abundance at high root rot infestation levels. The class is estimated using the UNITE database

$r^2 = 0.57$ vs. heritable OTUs $r^2 = 0.59$). Reducing the prediction parameters to those 60 OTUs (Suppl. Table 2) derived from PCA led to a notable decline in average prediction ability (r2 = 0.46, $p < 0.001$). However, when concentrating on the 21 OTUs identified by PCA and GWAS, the prediction ability rose to an average of 0.57 ("PCA selected OTUs with QTL", $p < 0.001$). We can summarize that a reduction from 1,238 OTU markers down to 21 selected OTU markers did not result in statistically different prediction abilities. These 21 OTUs consisted of five bacterial and 16 fungal OTUs. Two of the bacterial OTUs have been reported above (bOTU26 & bOTU28), while bOTU84 (*Acidovorax sp.*), bOTU39 (*Neorhizobium sp.*), and bOTU342 (*Myroides sp.*) have not. The 16 fungal OTUs fall into the genus of *Dactylonectria sp.* (10), *Chaetomium sp.* (3), *Microdochium sp.* (1), *Clonostachys sp.* (1), and *Thelonectria sp.* (1). In the next phase, we sought to minimize the number of OTU predictors for effective OTU marker-assisted breeding. Throughout ten cross-validation tests, bOTU28, bOTU84, and fOTU144 consistently ranked in the top 0.5 quantiles of the most influential variables within the regression models derived from 21 PCA-associated OTUs that displayed an observable QTL. After selecting these three OTUs, we reran the regression model to predict the root rot phenotype using only these OTUs. The average prediction ability we achieved was 0.41, which indicates a notable decrease in predictive performance compared to the full set of heritable OTUs ($p < 0.001$), underlining the constraints of simplifying the model to just a few predictors. Merging

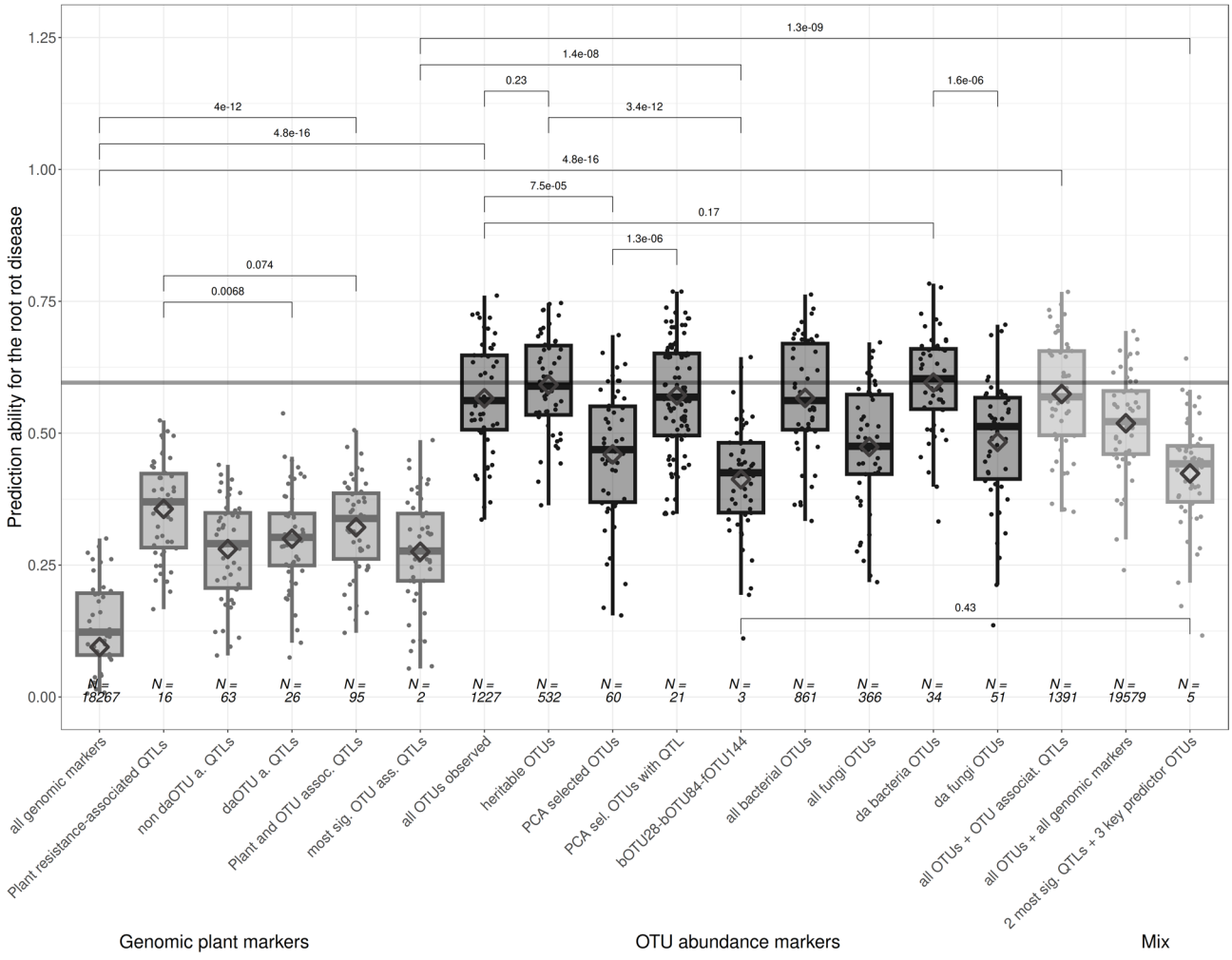

Fig. 7 Boxplots of the genomic prediction (phenotype forecast) correlation scores (predicted vs. measured in a dedicated test set) of the root rot index using either all available markers or a subset of these (e.g. QTLs) (6 left-sided boxplots, light gray background), OTUs as predictors (dark gray background), or a combination of both (3 right-sided boxplots). "N =" indicates the number of genomic markers or OTU markers used as predictors to estimate the root rot index in a Bayes-A or Bayes-B regression model. 5-fold cross validation with 10 replicates were performed for each set, highlighted by the dots. The brackets at the top present the pairwise comparisons derived *p*-values from a mean comparison. The gray horizontal line shows the highest average prediction ability across all predictor sets and ten cross-validations. The diamond shows the average prediction ability

the three chosen OTUs with the two most influential QTLs did not enhance the average prediction accuracy ($\mu = 0.42$, Fig. 7). Additionally, combining QTLs with OTU abundance values did not yield better predictions than using OTU abundance on its own.

Emergence

Similar outcomes were found in forecasting the emergence rate, showcasing a generally stronger predictive capability. The average prediction ability score across all cross-validations ranged from 0.46 to 0.76 (Suppl Fig. 1). Predictions using OTU markers are considerably greater than those using genomic (QTL) markers ($p < 0.001$). Additionally, QTL markers obtained from OTU abundances do not enhance predictions compared to those based on QTL markers derived from plant phenotypes. Finally, combined markers (genomic SNPs + OTU abundance) also increase predictions compared with genomic markers alone ($p < 0.001$) but do not further increase predictions compared with OTU markers. The overall best predictions were obtained by the PCA-selected OTUs with a QTL ($n = 21$, $\mu = 0.76$). Even though not significantly better than any other OTU-based predictions, the low number of 21 predictors makes them significantly more suitable for PCR-based assisted breeding than the other OTU sets. A further reduction to eight OTUs resulted in a significant decline of the prediction ability ($\mu = 0.68$, $p < 0.0001$). However, the set of eight OTUs differs significantly from the three OTUs chosen to predict the PRRC (only fOTU144 is similar; the other seven are all fOTUs), making the 21 PCA and QTL-derived

OTUs more universally applicable for predicting various phenotypes.

Discussion

The root rot complex is an important disease potentially resulting in total yield loss in pea cultivation [14]. The colonization and success of pathogens in infesting pea roots are highly dependent on the soil type and conditions (humidity and temperature) and the presence of other pathogens [45]. Besides, soils significantly vary in their ability to suppress pathogen colonization [46]. Although seed coating and fungicide applications can reduce the impact and development of negative microbiome composition, there is also a relevant genotype effect [15]. This indicates that some genotypes are more resistant to infections when grown in infested soil than others. Under sustainability aspects, genetic resistance is usually preferable to chemical plant protection [16].

Nevertheless, resistance towards PRRC has only been described as partial resistance [47]. It has also been shown that the efficacy of plant protection products is limited to control PRRC [48] and could harm positively acting microorganisms in the soil and root-like mycorrhiza [49].

Identification of heritable abundance of key taxa associated with PRRC

In general, we can report that more than 69% of the detected root microbial community abundance was genetically influenced by the pea genotypes, i.e., the genomic heritability is significantly higher than 0. Differential abundant OTUs showed higher heritabilities and a higher explained variance of the QTL markers. The highest heritability was observed for the fungi OTU285, annotated as a member of the family *Chaetomiaceae*, whose members have been reported to act as antagonists against phytopathogenic fungi, particularly *Fusarium oxysporum* and *Fusarium solani* [50, 51]. It has been shown to inhibit mycelial growth of *Fusarium sp.* by up to 35% and reduce conidial production of the pathogen by up to 76% [52], resulting in reduced *Fusarium* dissemination in the rhizosphere.

Furthermore, we found that OTUs related to *Dactylonectria* and *Fusarium* were the most common among the fungal OTUs with significant SNP markers for the genetically inherited abundance of these OTUs. Plenty of evidence describes different *Fusarium* species having negative physiological effects on pea [53–57]. We identified three different *Dactylonetria* associated OTUs with a genomic heritability of up to 0.44 and a negative correlation with root rot symptoms (Fig. 5). Up to six associated markers per OTU were identified at two different loci for the most significant *Dactylonectria* sp. related fOTU782 (chromosome 6 @85 MB, 95 MB, 265 MB). Although we found a positive correlation between *Dacytlonectria* abundance and plant health, no report has yet indicated any *Dactylonetria* species as a relevant collaborator with pea so far - it is rather known to be a plant pathogen with low host specificity [58–61].

We observed that the abundance of *Fusarium* annotated OTUs as genetically associated and can be attributed to the major QTL on chromosome 6 (Fig. 4A). Besides this major locus, we identified an additional QTL on the same chromosome (position 265 Mbp). The neighboring resistance QTL *Fsp-Ps2.1* against *F. solani* was also identified by Coyne et al. [54] in the same region of chromosome 6. Similarly, two QTLs for resistance to *Fusarium oxysporum* were identified on chromosome 6 in grass pea [62]. Another analysis for *Fusarium* root rot in pea found a QTL on chromosome 7. The reported QTL effect was rather weak and related to partial resistance to *Fusarium oxysporum* races 1 and 5 [63]. The *Fusarium vanettenii* annotated OTUs, which were found to be genetically heritable in our analyses ($h^2 > 0.21$ for 3 OTUs with identified QTLs), have so far only been described in tomato root rot. It may also be relevant in pea [64]. Furthermore, the abundance and presence of *Fusarium* are not only determined by genotype but also by environmental effects, such as soil moisture and compaction [56, 57].

Besides, we observed the bOTU26 and bOTU28 abundance to be positively correlated with the pea root rot infestation level (Suppl. Figure 2). Both OTUs were classified as *Stenotrophomonas* sp., from which the species *S. rhizophila* has been reported to have a promoting effect on plant growth and health – contrasting to our observations (Fig. 5) [65–67]. A QTL for both OTUs was found on chromosome 6 between 85 and 95 MB, the same region where the root rot, emergence, and biomass pea phenotypes were mapped. Together with a genomic heritability of 0.31 (bOTU26) and 0.12 (bOTU28), this highlights the fact that their abundance is genetically influenced by the pea genotype (Fig. 5). A similar promotion effect of tomato plants on *Stenotrophomonas* sp. in infested soils was reported by Berendsen et al. [68]. In the context of Berendsen et al., the significant positive correlation of disease intensity and *Stenotrophomonas* sp. abundance observed in our experiment might also be an indication for suppression of pathogens, if *Stenotrophomonas* sp. acts as antagonist to other soil borne pathogens. The same conclusion applies to the rhizobacterium bOTU63 (*Serratia fonticola* [100% BLAST identity], genomic heritability = 0.16). bOTU63 was observed to be the best explanatory variable for PRRC infestation in the PCA (Fig. 1). The abundance of bOTU63 was positively correlated with the root rot index ($r = 0.22$, $p < 0.01$, Suppl. Figure 2). In contrast to this observation, *Serratia fonticola* has been described as a plant growth-promoting

rhizobacterium by producing lytic enzymes against soil-borne fungal pathogens [69]. These contrasting observations underline the importance of functional validations to determine causalities in the plant-microbe interaction network.

The major locus on chromosome 6 could be associated with a range of OTUs

We found evidence for genomic regions in the pea genome associated with the abundance of different *Fusarium* and *Dactylonectria* taxa. These are associated with a major and intermediate QTL on chromosome 6 (position 85–95 & 265 MB). These QTLs also showed highly significant markers for the fungal beta diversity. The alpha diversity was not associated with any genomic locus for fungi or bacteria, suggesting that the pea genotype may not modulate the number of OTUs observed in the root under root rot stress. Besides, the number of QTLs was not significantly different between daOTUs and non-daOTUs.

The high number of detected QTLs on chromosome 6 in the genomic region from 85 to 95 MB indicates the high importance of the entire region for modulating the microbiome–plant interaction. Furthermore, a QTL for resistance to *Aphanomyces* root rot in pea, a pathogen also present in the root samples examined [70], was found together with a QTL for vigor in the same region, underlining the importance of this region for resistance to an important *Oomycetes* pathogen [71, 72]. In addition to these associations with resistance, this region on chromosome 6 also seems to influence fibre content [73] and NDVI under heat and drought stress [74]. Ultimately, significant associations with the phenotypic traits, emergence, shoot and root development, and root rot index were described for this region by Ariza-Suarez et al. [25].

Besides the main locus on chromosome 6, we identified 50 additional QTL (Suppl. Table 1). Similar numbers of QTLs have been identified in foxtail millet and tomato [75, 76]. It can be concluded that chromosome 6 is the most relevant genomic region in this diverse panel of genotypes studied for modulating resistance to a root rot infection. As shown by Ariza-Suarez et al. [25], the region is characterized by low linkage disequilibrium, making it easier to target specific loci and allele combinations in a breeding program. Nevertheless, the high number of 10 QTLs sub-regions (Fig. 4A) in the region on chromosome 6 makes prediction of potential candidate genes challenging. We conclude that several candidate genes from this region influence the microbial composition.

Prediction PRRC using genomic markers and OTU abundance

Compared to research applying genomic predictions in pea, the predictive ability is in a comparable range to genomic predictions on *Ascochyta* blight ($r = 0.56$) [77] or the seed number ($r = 0.4$–0.7) but inferior to predictions on the seed weight ($r = 0.8$–0.9) or flowering ($r = 0.7$) [78]. The root rot index prediction correlations showed a comparable range to the equivalently complex trait seed yield [79].

Across all genomic plant marker-based approaches, no statistically significant differences in the prediction ability could be detected. Nevertheless, it is remarkable that two single markers can equally well predict complex traits like the emergence rate or the root rot compared to the entire set of 18,267 markers. As previously shown, increasing the number of markers does not necessarily lead to an improved prediction power. The count and genomic composition of tested genotypes have a much higher relevance.

Likewise, when using the OTU abundance to predict the pea resistant phenotype, significantly higher prediction abilities were observed than all SNP marker-based approaches (r_{emerg}=0.71, r_{RRI}= 0.53; across all tested OTU combinations). Applying the OTU abundance instead of the SNP markers resulted, on average, in a 0.19 and 0.26 higher predictive ability for the emergence and root rot index, respectively ($p < 0.05$). Similarly, Gu et al. [80] highlighted the improved prediction ability of the microbiome on plant health. One reason for the lower prediction ability of genetic markers might be the genetic background of the tested pea lines. Based on the markers, we noticed two distinct groups in resistance related to the European and North American origin of these lines (Fig. 1B [25]). Further, the plant phenotype might be modulated by microorganisms that are not associated with plant genetics. A microbe's abundance might depend on the pea genotype and the competition or symbiotic interactions in the root. Some key microbes relevant for plant health might not directly be determined by the plant genotype but interact with other microbes, which abundance is modulated by the plant genotype (indirect effects). As the combination of markers and OTU abundance levels did not improve the prediction ability, we assume that the QTLs already carry redundant information in the OTU abundance.

The predictions could be further improved by adding some selected markers to the two QTLs into the genomic prediction model, as proposed in the GMStool [81]. Still, adding dozens of additional markers might lead to reduced applicability in marker-assisted breeding. Therefore, we focused on the OTUs and used a comparable approach, and selected the most relevant OTUs by PCA and QTL mapping filtering. The abundance of these OTUs was used in a phenotype forecast framework. It resulted in prediction accuracies of up to 0.81 for emergence and the root rot index using 21 OTUs as predictors (Fig. 7, Suppl. Figure 1, Suppl. Table 2, "PCA + QTL

derived OTUs"). Therefore, we want to stress that feature (genomic marker, OTU abundance) selection can be of value to retain similar prediction accuracies with significantly reduced predictor features.

Application in breeding resistant pea lines

In terms of breeding more resistant genotypes towards root rot resistance, the detected OTU markers can be used in marker-assisted selection to select genotypes with a desirable phenotype. Besides, the abundance of relevant OTUs could also be used as markers for a marker-assisted selection (MAS) approach. Instead of testing the entire microbiome, PCR primers specific to key microbial markers could be generated to reduce sequencing costs. Nevertheless, the effort of collecting the samples for microbiome analysis and processing the collected data is an additional cost factor and potentially error-prone due to sampling deviations. Although a previous study did not find a significant correlation between highly abundant *A. euteiches* and pea root rot disease parameters [70], the examination of *Oomycetes* might be suitable to complement resistance prediction accuracies [82]. Here, we demonstrated that a holobiont-based approach can enhance selection efficiency and success for PRRC-resistant genotypes.

Conclusion

The obtained findings indicate that (i) the abundance of certain microbes is influenced by the pea genotype and can be attributed to specific genomic loci (QTLs); (ii) root rot resistance is associated with the holobiont, i.e. by the plant, its associated microbiome and complex interactions within the microbiome; and (iii) the holobiont-based genomic analyses and derived markers for plant resistance and recruitment of root microorganisms lead to an increased prediction ability of plant health compared to plant genetic markers as single source. This study identifies potential breeding applications for microbiome-assisted disease resistance.

Supplementary Information

The online version contains supplementary material available at https://doi.org/10.1186/s12870-025-06995-9.

Supplementary Material 1: Suppl. Table 1: List of all detected QTLs across all OTUs and phenotypes above the significance threshold for the respective group. Besides the genomic position, the LOD value and the respective OTU are listed. Supple Table 2: OTUs selected based on a PCA for OTU-based genomic predictions for phenotype predictions of root rot index (RRI) and emergence rate. For OTUs colored in green we detected a QTL.

Supplementary Material 2: Suppl. Figure 1. Boxplots of the genomic prediction (phenotype forcast) correlation scores (predicted vs. measured in a dedicated test set) of the ***emergence rate*** using either all available markers or a subset of these (e.g. QTLs) (6 left-sided boxplots, light gray background), OTUs as predictors (dark gray background), or a combination of both (3 right-sided boxplots). "N =" indicates the number of genomic markers or OTU markers used as predictors to estimate the root rot index in a Bayes-A or Bayes-B regression model. 5-fold cross validation with 10 replicates were performed for each set, highlighted by the dots. The brackets at the top present the pairwise comparisons derived ***p***-values from a mean comparison. The gray horizontal line shows the highest average prediction ability across all predictor sets and ten cross-validations. Suppl. Figure 2. Pearson correlation (r) of annotated OTUs to the pea root rot index. OTUs were annotated to species or genus by BLAST. The number on the species' right or genus name indicates the number of matched OTUs. The coloring of species or genus names illustrates the negative (red) or positive (green) correlation with the root rot index (RRI). The color in the lollipop plot indicates the BLAST identity to the most similar NCBI database organism. The value in the circle shows the narrow-sense genomic heritability. Fungi (A) and Bacteria (B) are separated in subplots. The arrow indicates the highest narrow-sense genomic heritability per group. Suppl. Figure 3. Pearson correlation of OTUs with a genomic heritability above 0.15. Correlations have been calculated separately for low-infected (A) and highly-infected (B) genotypes. Boxes indicate selected OTUs, based on the previous analysis.

Acknowledgements

We thank the Genetic Diversity Centre at ETH Zurich for their contribution to processing the raw sequencing reads.

Authors' contributions

MMM, PH, and BS designed research. LW performed research. MS and VG analyzed data with input from MH, NB, DAS, KO, BS, PH, and MMM. MS wrote the first draft of the manuscripts. All coauthors contributed to the internal revision process of the manuscript. All authors approved the final version of the paper.

Funding

This study was conducted in the framework of the EU projects LIVESEED (EU HORIZON2020 contract no. 727230, and by the Swiss State Secretariat for Education, Research and Innovation (SERI) under contract no. 17.0009 and Root2Res (EU Horizon Europe no. 101060124 and Swiss State Secretariat for Education, Research and Innovation (SERI) no 23.00050) and the Gebert Rüf Foundation (GRS-082/19) and MICIU/AEI/10.13039/501100011033 and FSE+ under grant reference no RYC2022-037997-I. The opinions expressed and arguments employed herein do not necessarily reflect the official views of the EC and the Swiss government. Neither the European Commission/SERI nor any person acting behalf of the Commission/SERI is responsible for the use which might be made of the information provided on this publication.

Data availability

The raw sequencing datasets are available in the European Nucleotide Archive (ENA, http://www.ebi.ac.uk/ena) at EMBL-EBI under the study accession PRJEB83630.

Declarations

Ethics approval and consent to participate

Not applicable.

Consent for publication

Not applicable.

Competing interests

The authors declare no competing interests.

Author details

[1]Research Institute of Organic Farming (FiBL), Frick, Switzerland
[2]Molecular Plant Breeding, Institute of Agricultural Sciences, ETH Zurich, Zürich, Switzerland
[3]KWS LOCHOW GmbH, Bergen, Germany
[4]Department of Environmental Systems Science, Sustainable Agroecosystems Group, ETH Zurich, Zürich, Switzerland
[5]Department of Biology, Healthcare and the Environment, Faculty of Pharmacy and Food Sciences, Universitat de Barcelona, Barcelona, Spain

Received: 19 May 2025 / Accepted: 30 June 2025
Published online: 09 August 2025

References

1. Foyer CH, Nguyen H, Lam HM. Legumes—the art and science of environmentally sustainable agriculture. Plant Cell Environ. 2019;42(1):1–5.
2. Hemler EC, Hu FB. Plant-Based diets for personal, population, and planetary health. Adv Nutr. 2019;10(Supplement4):S275–83.
3. FAOSTAT. 2023. Available from: https://www.fao.org/faostat/en/#data/QCL. [cited 2023 Jun 30].
4. Jensen ES. Seasonal patterns of growth and nitrogen fixation in field-grown pea. Plant Soil. 1987;101(1):29–37.
5. Borisov AY, Danilova TN, Koroleva TA, Kuznetsova EV, Madsen L, Mofett M, et al. Regulatory genes of garden pea (*Pisum sativum* L.) controlling the development of nitrogen-fixing nodules and arbuscular mycorrhiza: a review of basic and applied aspects. Appl Biochem Microbiol. 2007;43(3):237–43.
6. Jha AB, Gali KK, Alam Z, Lachagari VBR, Warkentin TD, Jha AB, et al. Potential application of genomic technologies in breeding for fungal and oomycete disease resistance in pea. Agron 2021. 2021;11(6):1260.
7. Wille L, Messmer MM, Bodenhausen N, Studer B, Hohmann P. Heritable variation in pea for resistance against a root rot complex and its characterization by amplicon sequencing. Front Plant Sci. 2020;11. Available from: https://www.frontiersin.org/journals/plant-science/articles/10.3389/fpls.2020.542153.
8. Xue AG. Biological control of pathogens causing root rot complex in field pea using *Clonostachys rosea* strain ACM941. Phytopathology. 2003;93(3):329–35.
9. Bani M, Rubiales D, Rispail N. A detailed evaluation method to identify sources of quantitative resistance to *fusarium oxysporum* f. sp. *pisi* race 2 within a *pisum* sp.. germplasm collection. Plant Pathol. 2012;61(3):532–42.
10. Kraft JM, Pfleger FL. Compendium of pea diseases and pests. 2001. Available from: https://blackwells.co.uk/bookshop/product/Compendium-of-Pea-Diseases-and-Pests-by-John-M-Kraft-Francis-Louis-Pfleger-American-Phytopathological-Society/9780890542699. [cited 2025 Apr 17].
11. Wille L, Messmer MM, Studer B, Hohmann P. Insights to plant–microbe interactions provide opportunities to improve resistance breeding against root diseases in grain legumes. Plant Cell Environ. 2019;42(1):20–40.
12. Sivachandra Kumar NT, Cox,Laura A-C, Cheryl, and, Banniza S. Optimization of zoospore production and inoculum concentration of Aphanomyces euteiches for resistance screening of pea and lentil. Can J Plant Pathol. 2020;42(3):419–28.
13. Mathew FM, Lamppa RS, Chittem K, Chang YW, Botschner M, Kinzer K, et al. Characterization and pathogenicity of *Rhizoctonia solani* isolates affecting *Pisum sativum* in North Dakota. Plant Dis. 2012;96(5):666–72.
14. Williamson-Benavides BA, Dhingra A. Understanding root rot disease in agricultural crops. Horticulturae. 2021;7(2):33.
15. Wohor OZ, Rispail N, Ojiewo CO, Rubiales D. Pea breeding for resistance to rhizospheric pathogens. Plants. 2022;11(19):2664.
16. Sharma A, Rani M, Lata H, Thakur A, Sharma P, Kumar P, et al. Global dimension of root rot complex in garden pea: current status and breeding prospective. Crop Prot. 2022;158:106004.
17. Rubiales D, Fondevilla S, Chen W, Gentzbittel L, Higgins TJV, Castillejo MA, et al. Achievements and challenges in legume breeding for pest and disease resistance. Crit Rev Plant Sci. 2015;34(1–3):195–236.
18. Hassani MA, Durán P, Hacquard S. Microbial interactions within the plant holobiont. Microbiome. 2018;6(1):58.
19. Delaux PM, Schornack S. Plant evolution driven by interactions with symbiotic and pathogenic microbes. Science. 2021;371(6531):eaba6605.
20. Van den Koornhuyse P, Quaiser A, Duhamel M, Le Van A, Dufresne A. The importance of the microbiome of the plant holobiont. New Phytol. 2015;206(4):1196–206.
21. Deng S, Caddell DF, Xu G, Dahlen L, Washington L, Yang J, et al. Genome wide association study reveals plant loci controlling heritability of the rhizosphere microbiome. ISME J. 2021;15(11):3181–94.
22. Escudero-Martinez C, Coulter M, Alegria Terrazas R, Foito A, Kapadia R, Pietrangelo L, et al. Identifying plant genes shaping microbiota composition in the barley rhizosphere. Nat Commun 2022 131. 2022;13(1):1–14.
23. Mendes LW, Mendes R, Raaijmakers JM, Tsai SM. Breeding for soil-borne pathogen resistance impacts active rhizosphere microbiome of common bean. ISME J. 2018;12(12):3038.
24. Gfeller V, Schneider M, Bodenhausen N, et al. Crop genotype modulates root rot resistance-associated microbial community composition and abundance of key taxa. Environ Microbiome. 2025;20:89. https://doi.org/10.1186/s40793-025-00755-w
25. Ariza-Suarez D, Wille L, Hohmann P, Gfeller V, Schneider M, Horton M et al. Association genetics and genomic prediction for resistance to root rot in a diverse collection of Pisum sativum L. 2024. Available from: https://www.authorea.com/users/825782/articles/1221265-association-genetics-and-genomic-prediction-for-resistance-to-root-rot-in-a-diverse-collection-of-pisum-sativum-l?commit=5d2727db7e24a8c1f9f187a96edce09084285309. [cited 2025 Jan 30].
26. Yang T, Liu R, Luo Y, Hu S, Wang D, Wang C, et al. Improved pea reference genome and pan-genome highlight genomic features and evolutionary characteristics. Nat Genet. 2022;54(10):1553–63.
27. Langmead B, Salzberg SL. Fast gapped-read alignment with bowtie 2. Nat Methods. 2012;9(4):357–9.
28. Tello D, Gil J, Loaiza CD, Riascos JJ, Cardozo N, Duitama J. NGSEP3: accurate variant calling across species and sequencing protocols. Bioinformatics. 2019;35(22):4716–23.
29. Browning BL, Tian X, Zhou Y, Browning SR. Fast two-stage phasing of large-scale sequence data. Am J Hum Genet. 2021;108(10):1880–90.
30. Edgar RC. UNOISE2: improved error-correction for Illumina 16S and ITS amplicon sequencing. bioRxiv. 2016. p. 081257. Available from: https://www.biorxiv.org/content/10.1101/081257v1. [cited 2025 Jan 31].
31. Edgar RC. UPARSE: highly accurate OTU sequences from microbial amplicon reads. Nat Methods. 2013;10(10):996–8.
32. Nilsson RH, Larsson KH, Taylor AFS, Bengtsson-Palme J, Jeppesen TS, Schigel D, et al. The UNITE database for molecular identification of fungi: handling dark taxa and parallel taxonomic classifications. Nucleic Acids Res. 2019;47(D1):D259–64.
33. Bolyen E, Rideout JR, Dillon MR, Bokulich NA, Abnet CC, Al-Ghalith GA, et al. Reproducible, interactive, scalable and extensible microbiome data science using QIIME 2. Nat Biotechnol. 2019;37(8):852–7.
34. Callahan BJ, McMurdie PJ, Rosen MJ, Han AW, Johnson AJA, Holmes SP. DADA2: High-resolution sample inference from illumina amplicon data. Nat Methods. 2016;13(7):581–3.
35. Rognes T, Flouri T, Nichols B, Quince C, Mahé F. VSEARCH: a versatile open source tool for metagenomics. PeerJ. 2016;4:e2584.
36. Quast C, Pruesse E, Yilmaz P, Gerken J, Schweer T, Yarza P, et al. The SILVA ribosomal RNA gene database project: improved data processing and web-based tools. Nucleic Acids Res. 2013;41(Database issue):D590–596.
37. Camacho C, Coulouris G, Avagyan V, Ma N, Papadopoulos J, Bealer K, et al. BLAST+: architecture and applications. BMC Bioinformatics. 2009;10(1):421.
38. Sayers EW, Bolton EE, Brister JR, Canese K, Chan J, Comeau DC, et al. Database resources of the National center for biotechnology information. Nucleic Acids Res. 2022;50(D1):D20–6.
39. Fernandes AD, Reid JN, Macklaim JM, McMurrough TA, Edgell DR, Gloor GB. Unifying the analysis of high-throughput sequencing datasets: characterizing RNA-seq, 16S rRNA gene sequencing and selective growth experiments by compositional data analysis. Microbiome. 2014;2:15.
40. Mantel N. The detection of disease clustering and a generalized regression approach. Cancer Res. 1967;27(2):209–20.
41. Oksanen J, Simpson GL, Blanchet FG, Kindt R, Legendre P, Minchin PR et al. vegan: community ecology package. 2025. Available from: https://cran.r-project.org/web/packages/vegan/index.html. [cited 2025 Jun 18].
42. Endelman J. rrBLUP: ridge regression and other kernels for genomic selection. 2023. Available from: https://cran.r-project.org/web/packages/rrBLUP/index.html. [cited 2025 Apr 17].
43. Horton MW, Bodenhausen N, Beilsmith K, Meng D, Muegge BD, Subramanian S, et al. Genome-wide association study of *Arabidopsis thaliana* leaf microbial community. Nat Commun. 2014;5(1): 5320.
44. Pérez P, de los Campos G. Genome-wide regression and prediction with the BGLR statistical package. Genetics. 2014;198(2):483–95.
45. Chatterton S, Schwinghamer TD, Pagé A, Davidson RB, Harding MW, Banniza S. Inoculum dose–disease response relationships for the pea root rot pathogen, Aphanomyces euteiches, are dependent on soil type and other pathogens. Front Plant Sci. 2023;14. Available from: https://www.frontiersin.org; https://www.frontiersin.org. [cited 2025 Apr 17].
46. Persson L, Larsson-Wikström M, Gerhardson B. Assessment of soil suppressiveness to *aphanomyces* root rot of pea. Plant Dis. 1999;83(12):1108–12.
47. Porter LD, Kraft JM, Grünwald NJ. Release of pea germplasm with fusarium resistance combined with desirable yield and Anti-Lodging traits. J Plant Regist. 2014;8(2):191–4.

48. Nazir N, Badri ZA, Bhat NA, Bhat FA, Sultan P, Bhat TA, et al. Effect of the combination of biological, chemical control and agronomic technique in integrated management pea root rot and its productivity. Sci Rep. 2022;12(1):11348.
49. Singh G, Wright D. In vitro studies on the effects of herbicides on the growth of rhizobia. Lett Appl Microbiol. 2002;35(1):12–6.
50. Galindo Flores H, Martínez Álvarez JC, Nava Pérez E, García Estrada RS, Maldonado Mendoza IE. A saprotrophic fungal isolate from Northern Sinaloa, Mexico, with homology to members of the chaetomiaceae behaves as an antagonist of phytopathogenic fungi in vitro. 2005. Available from: http://www.repositoriodigital.ipn.mx//handle/123456789/8591. [cited 2024 Apr 22].
51. Abo-Elyousr KAM, Ibrahim OHM, Al-Qurashi AD, Mousa MAA, Saad MM. Biocontrol potential of endophytic fungi for the Eco-Friendly management of root rot of cuminum cyminum caused by fusarium Solani. Agron 2022. 2022;12(11):2612. 12 Page 2612.
52. Phong NH, Pongnak W, Soytong K. Antifungal activities of *Chaetomium* spp. against fusarium wilt of tea. Plant Prot Sci. 2016;52(1):10–7.
53. Kerr A. The root rot-fusarium wilt complex of peas. Aust J Biol Sci. 1963;16(1):55–69.
54. Coyne CJ, Porter LD, Boutet G, Ma Y, McGee RJ, Lesné A, et al. Confirmation of fusarium root rot resistance QTL Fsp-Ps 2.1 of pea under controlled conditions. BMC Plant Biol. 2019;19(1):1–8.
55. Bodah ET, Porter LD, Chaves B, Dhingra A. Evaluation of pea accessions and commercial cultivars for fusarium root rot resistance. Euphytica. 2016;208(1):63–72.
56. Kraft JM, Boge W. Root characteristics in pea in relation to compaction and fusarium root rot. Plant Dis. 2001;85(9):936–40.
57. Tu JC. Effects of soil compaction, temperature, and moisture on the development of the fusarium root rot complex of pea in southwestern Ontario. Phytoprotection. 1994;75(3):125–31.
58. Auger J, Pérez I, Esterio M. Occurrence of root rot disease of Cherimoya (*Annona cherimola* Mill.) caused by *dactylonectria macrodidyma* in Chile. Plant Dis. 2015;99(9):1282–1282.
59. Manici LM, Caboni E, Caputo F, Frattarelli A, Lucioli S. Phytotoxins from *Dactylonectria torresensis* involved in replant disease of fruit trees. Rhizosphere. 2021;17:100300.
60. Nigro F, Antelmi I, Sion V, Parente P, Pacifico A. First report of *dactylonectria torresensis* causing foot and root rot of olive trees. Plant Dis. 2019;103(4):768–768.
61. Weber RWS, Entrop AP. *Dactylonectria torresensis* as the main component of the black root rot complex of strawberries and raspberries in Northern Germany. Erwerbs-Obstbau. 2017;59(3):157–69.
62. Sampaio AM, Alves ML, Pereira P, Valiollahi E, Santos C, Šatović Z, et al. Grass pea natural variation reveals oligogenic resistance to fusarium oxysporum f. Sp. pisi. Plant Genome. 2021;14(3):e20154.
63. Feng J, Hwang R, Chang KF, Conner RL, Hwang SF, Strelkov SE, et al. Identification of microsatellite markers linked to quantitative trait loci controlling resistance to fusarium root rot in field pea. Can J Plant Sci. 2011;91(1):199–204.
64. Debbarma R, Kamil D, Maya Bashyal B, Choudhary SP, Thokla P. First report of root rot disease on solanum lycopersicum L. caused by fusarium Vanettenii in India. J Phytopathol. 2021;169(11–12):752–6.
65. Alavi P, Starcher MR, Zachow C, Müller H, Berg G. Root-microbe systems: the effect and mode of interaction of stress protecting agent (SPA) Stenotrophomonas rhizophila DSM14405T. Front Plant Sci. 2013;4:51567.
66. Egamberdieva D, Jabborova D, Berg G. Synergistic interactions between *Bradyrhizobium japonicum* and the endophyte *Stenotrophomonas rhizophila* and their effects on growth, and nodulation of soybean under salt stress. Plant Soil. 2016;405(1–2):35–45.
67. Schmidt CS, Alavi M, Cardinale M, Müller H, Berg G. *Stenotrophomonas rhizophila* DSM14405T promotes plant growth probably by altering fungal communities in the rhizosphere. Biol Fertil Soils. 2012;48(8):947–60.
68. Berendsen RL, Vismans G, Yu K, Song Y, de Jonge R, Burgman WP, et al. Disease-induced assemblage of a plant-beneficial bacterial consortium. ISME J. 2018;12(6):1496–507.
69. Kshetri L, Naseem F, Pandey P. Role of Serratia sp. as biocontrol agent and plant growth stimulator, with prospects of biotic stress management in plant. In: Sayyed RZ, editor. Plant growth promoting rhizobacteria for sustainable stress management: Volume 2: Rhizobacteria in Biotic Stress Management. Singapore: Springer; 2019. pp. 169–200. Available from: https://doi.org/10.1007/978-981-13-6986-5_6. [cited 2025 Apr 17].
70. Wille L, Kurmann M, Messmer MM, Studer B, Hohmann P. Untangling the pea root rot complex reveals microbial markers for plant health. Front Plant Sci. 2021;12. Available from: https://www.frontiersin.org/journals/plant-science/articles/10.3389/fpls.2021.737820.
71. PulseDB. 2025. Available from: https://www.pulsedb.org/. [cited 2025 Apr 17].
72. Wu L, Fredua-Agyeman R, Hwang SF, Chang KF, Conner RL, McLaren DL, et al. Mapping QTL associated with partial resistance to aphanomyces root rot in pea (*Pisum sativum* L.) using a 13.2 K SNP array and SSR markers. Theor Appl Genet. 2021;134(9):2965–90.
73. Gali KK, Sackville A, Tafesse EG, Lachagari VBR, McPhee K, Hybl M, et al. Genome-wide association mapping for agronomic and seed quality traits of field pea (Pisum sativum L.). Front Plant Sci. 2019;10. Available from: https://www.frontiersin.org; https://www.frontiersin.org. [cited 2025 Apr 17].
74. Tafesse EG, Gali KK, Lachagari VBR, Bueckert R, Warkentin TD. Genome-wide association mapping for heat and drought adaptive traits in pea. Genes. 2021;12(12):1897.
75. Wang Y, Wang X, Sun S, Jin C, Su J, Wei J, et al. GWAS, MWAS and mGWAS provide insights into precision agriculture based on genotype-dependent microbial effects in Foxtail millet. Nat Commun 2022 131. 2022;13(1):1–17.
76. Oyserman BO, Flores SS, Griffioen T, Pan X, van der Wijk E, Pronk L, et al. Disentangling the genetic basis of rhizosphere microbiome assembly in tomato. Nat Commun. 2022;13(1):3228.
77. Carpenter MA, Goulden DS, Woods CJ, Thomson SJ, Kenel F, Frew TJ, et al. Genomic selection for ascochyta blight resistance in pea. Front Plant Sci. 2018;9. Available from: https://www.frontiersin.org; https://www.frontiersin.org. [cited 2025 Apr 17].
78. Burstin J, Salloignon P, Chabert-Martinello M, Magnin-Robert JB, Siol M, Jacquin F, et al. Genetic diversity and trait genomic prediction in a pea diversity panel. BMC Genomics. 2015;16(1):105.
79. Bari MAA, Zheng P, Viera I, Worral H, Szwiec S, Ma Y, et al. Harnessing genetic diversity in the USDA pea germplasm collection through genomic prediction. Front Genet. 2021;12. Available from: https://www.frontiersin.org; https://www.frontiersin.org. [cited 2025 Apr 17].
80. Gu Y, Banerjee S, Dini-Andreote F, Xu Y, Shen Q, Jousset A, et al. Small changes in rhizosphere microbiome composition predict disease outcomes earlier than pathogen density variations. ISME J. 2022;16(10):2448–56.
81. Jeong S, Kim JY, Kim N, GMStool. GWAS-based marker selection tool for genomic prediction from genomic data. Sci Rep. 2020;10(1):19653.
82. Desgroux A, L'Anthoëne V, Roux-Duparque M, Rivière JP, Aubert G, Tayeh N, et al. Genome-wide association mapping of partial resistance to *aphanomyces euteiches* in pea. BMC Genomics. 2016;17(1):124.

Publisher's Note